ELSEVIER

International Journal of Mass Spectrometry 184 (1999) 183–189

International Journal of Mass Spectrometry

The thermochemistry of formic acid–halide anion clusters

Barry W. Walker, Lee S. Sunderlin*

Department of Chemistry, Northern Illinois University, DeKalb, IL 60115, USA

Received 3 November 1998; accepted 5 January 1999

Abstract

Bond dissociation energies for formic acid–halide ion clusters have been measured using energy-resolved collision-induced dissociation in a flowing afterglow-tandem mass spectrometer. The resulting 0 K bond energies (in kJ mol^{-1}) are $D(HCOOH–X^-) = 114 \pm 9$, 70 ± 7, and 52 ± 9 for X = Cl, Br, and I, respectively. The second bond energies are $D[(HCOOH)X^-–HCOOH] = 50 \pm 9$, 43 ± 7, and 45 ± 9, respectively. These results are compared to empirical correlations, semiempirical calculations, and previously determined values where available. (Int J Mass Spectrom 184 (1999) 183–189) © 1999 Elsevier Science B.V.

Keywords: Hydrogen bonding; Halide affinity; Flowing afterglow

1. Introduction

Understanding the complexation of individual solvent molecules to ions is a key step in understanding bulk ion solvation [1,2], nucleation phenomena [3,4], and hydrogen bonding [5,6]. Because of this, the energetics of binding a small number of solvent molecules to ions in the gas phase have been extensively studied [7,8]. The halide anions [9] and alkali cations [10] are often used to explore periodic trends of solvation because of their simple closed-shell electronic structures and spherical symmetry. For example, these ions were anchors for the Born Model of bulk ion solvation [11] and variations on this model [1,12]. Another advantage of the halides as a model system is that, with the exception of fluoride, they are very weak Arrhenius bases that do not abstract a proton from the solvent unless the solvent is a strong acid. Halide affinities also have applications in predicting the results of chemical ionization experiments [13]. Several groups have studied the bonding of halides to neutral compounds such as H_2O [14], CH_3OH [15], alcohols [16,17], SO_2 [18], and HF [19].

Hydrogen bonding involving carboxylic acids is of particular biological importance, and formic acid is the simplest carboxylic acid. Previous gas-phase studies by Kebarle and co-workers [20–22], Larson and McMahon [23], and Meot-ner and Sieck [24] indicate that formic acid can form strong hydrogen bonds with anions. Łuczynski, Włodek, and Wincel [25] reported remarkably strong bond energies for $(HCOOH)_yCl^-$ ($y = 2–5$) clusters. However, bond energies for $(HCOOH)Br^-$ and most of the larger clusters are not known. This study measures a complete set of solvation energies for $(HCOOH)_yX^-$ ($y = 1$ and 2) complexes in order to clarify the periodic trends.

Fluoride complexes with formic acid are not inves-

* Corresponding author. E-mail: sunder@niu.edu

PII S1387-3806(99)00008-1

tigated in this work because HF is actually a weaker acid than formic acid in the gas phase. Therefore, such clusters are more appropriately viewed as $HCOO^-$–HF [26].

2. Experimental

The formic acid–halide cluster bond strengths were measured using energy-resolved collision-induced dissociation in a flowing afterglow-tandem mass spectrometer (MS) [27]. The instrument consists of an ion source region, a flow tube, and the tandem MS. The dc discharge ion source used in these experiments is typically set at 800 V with 0.5 mA of emission current. The flow tube is a 92 cm × 7.3 cm inner diameter (i.d.) stainless steel pipe that operates at a buffer gas pressure of 0.4 Torr and flow rate of 200 standard cm^3/s. The buffer gas is helium with up to 5% argon added to stabilize the dc discharge. Approximately 10^5 collisions with the buffer gas cool the ions to room temperature.

To make the $(HCOOH)_yX^-$ cluster ions for this study, halide ions were first formed by adding appropriate precursors to the ion source. Formic acid was then added further downstream in the flow tube. Metastable $(HCOOH)_yX^-$ complexes were cooled by collisions with the buffer gas. Water was introduced at the ionization source as a chaperone molecule to improve the efficiency of clustering; this increased the intensities of the desired ions by factors of up to 80 under optimized conditions. The halide precursors used in the experiments were chloroform, *n*-bromopropane, and iodine. These precursors were chosen because they have convenient vapor pressures at room temperature and do not lead to interferences at the ion masses studied.

The tandem MS includes a quadrupole mass filter, an octopole ion guide, a second quadrupole mass filter, and a detector, which are contained in a stainless steel box that is partitioned into five interior chambers. Differential pumping on the five chambers ensures that further collisions of the ions with the buffer gas are unlikely after ion extraction. During the collision-induced dissociation (CID) experiments, the ions are extracted from the flow tube and focused into the first quadrupole (Q1) for mass selection. The reactant ions from Q1 are then focused into the octopole, which passes through a reaction cell that contains argon as a collision gas. After the dissociated and unreacted ions pass through the reaction cell, the second quadrupole is used for mass analysis. The detector is an electron multiplier operating in pulse-counting mode.

In CID, the energy threshold for a reactant ion is determined by modeling the intensity of the product ions as a function of the reactant ion kinetic energy in the center-of-mass (c.m.) frame E_{cm}. The octopole is used as a retarding field analyzer when the reactant ion beam energy zero is measured. The ion kinetic energy distribution is typically Gaussian with a full width at half maximum of 0.6–1.2 eV (1 eV = 96.4 kJ mol^{-1}). The octopole offset voltage measured with respect to the center of the Gaussian fit gives the laboratory kinetic energy E_{lab} in eV. Truncation of the ion beam at low offset energies is corrected for [28a,b]. To convert to the c.m. frame, the equation $E_{cm} = E_{lab}m/(m + M)$ is used, where m and M are the masses of the neutral and ionic reactants, respectively.

All experiments involving chloride and bromide were performed with Q1 at a sufficiently high resolution to transmit only one isotopic peak. The ^{35}Cl, ^{37}Cl, ^{79}Br, ^{81}Br, and ^{127}I isotopes were all used for different experiments. No differences between two isotopes of the same element were observed. The final mass filter was operated at low resolution in order to improve ion collection efficiency.

The total cross section for a reaction σ_{total} is calculated using Eq. (1), where I is the intensity of the reactant ion beam, I_0 is the intensity of the incoming beam ($I_0 = I + \Sigma I_i$), I_i is the intensity of each product ion, n is the number density of the collision gas, and l is the effective collision length, 13 ± 2 cm. Individual product cross sections σ_i are equal to $\sigma_{total}(I_i/\Sigma I_i)$.

$$I = I_0 \exp(-\sigma_{total} n l) \quad (1)$$

A threshold energy is derived by fitting the data to a model function given in Eq. (2), where $\sigma(E)$ is the cross section for formation of the product ion at c.m. energy E, E_T is the desired threshold energy, σ_0 is the scaling factor, n is an adjustable parameter, and i denotes rovibrational states having energy E_i and population g_i ($\Sigma g_i = 1$). Doppler broadening and the kinetic energy distribution of the reactant ion are also accounted for in the data analysis, which is done using the CRUNCH program written by Armentrout and coworkers [28].

$$\sigma(E) = \sigma_0 \sum_i g_i(E + E_i - E_T)^n/E \quad (2)$$

Many of the necessary vibrational frequencies are not known, and high-level *ab initio* calculations on the larger systems are not currently practical [29]. Therefore, to ensure consistency, vibrational frequencies for all of the complexes were calculated using the AM1 semiempirical method and the PC-SPARTAN software package [30]. Bond enthalpies were also taken from AM1 calculations performed using PC-SPARTAN. Rotational constants for these complexes are derived from calculated geometries. The AM1 frequencies compare well to the experimental frequencies [31] for formic acid, with an average deviation of $-4 \pm 8\%$. Uncertainties in the internal energy content were estimated by multiplying the entire sets of frequencies by 0.9 and 1.1; the resulting changes in internal energies are only 1–2 kJ mol^{-1}.

In many cases, collisionally activated metastable complexes can have sufficiently long lifetimes that they do not dissociate on the experimental timescale ($\sim$30 μs). This leads to a "kinetic shift" in the observed threshold. The calculated effects for the present systems are 0–1 kJ mol^{-1} if it is assumed that the dissociation transition state is implausibly tight (a reactant-like transition state with an activation entropy near zero). The calculated kinetic shift is even lower if it is assumed that the transition state is very loose (a product-like transition state with a positive activation entropy). Thus, kinetic shifts are not significant in the present experiments.

An ion not sufficiently energized by one collision with the target gas may gain enough energy in a second collision to be above the dissociation threshold. This effect is eliminated by linear extrapolation of the data taken at several pressures to a zero pressure cross section before fitting the data [32a,b].

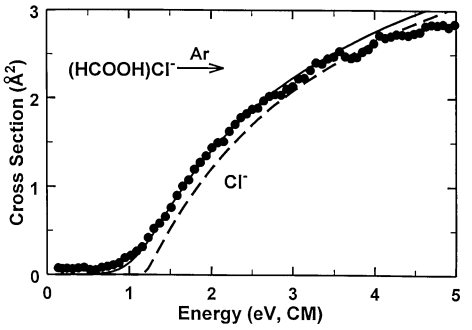

Fig. 1. Cross section for collision-induced dissociation of (HCOOH)Cl$^-$ as a function of energy in the center-of-mass frame. The solid line is the optimized fit to the data, and the dashed line is the fit without internal energy effects or translational energy broadening. See text for discussion of fitting procedures.

3. Results

In the flowing afterglow, the largest clusters detected are $(HCOOH)_4Cl^-$, $(HCOOH)_2Br^-$, and $(HCOOH)_2I^-$. Under higher pressure conditions, Łuczynski et al. [25] also observed $(HCOOH)_5Cl^-$. No other studies have reported data on $(HCOOH)_yX^-$ clusters with $y > 1$.

In the case of the $(HCOOH)X^-$ complexes, the loss of formic acid is observed as the only CID product except for X = Cl, where a small trace (less than 1%) of $HCOO^-$ is also seen. $(HCOOH)_2X^-$ primarily loses a single formic acid molecule, but the loss of two formic acid molecules is also seen at higher energies. The reaction channels observed are given in reactions (3)–(6), and appearance curves for the CID products of the formic acid–halide complexes studied are shown in Figs. 1–6.

$$(HCOOH)X^- \rightarrow HCOOH + X^- \quad (3)$$

$$(HCOOH)Cl^- \rightarrow HCOO^- + HCl \quad (4)$$

$$(HCOOH)_2X^- \rightarrow HCOOH + (HCOOH)X^- \quad (5)$$

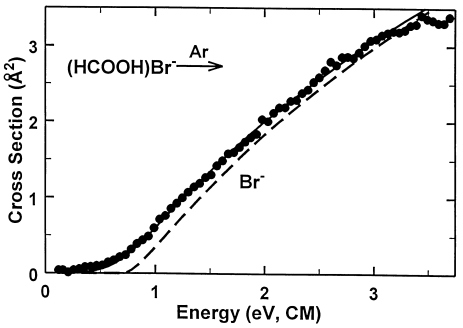

Fig. 2. Cross section for collision-induced dissociation of $(HCOOH)Br^-$ as a function of energy in the center-of-mass frame. The solid line is the optimized fit to the data, and the dashed line is the fit without internal energy effects or translational energy broadening. See text for discussion of fitting procedures.

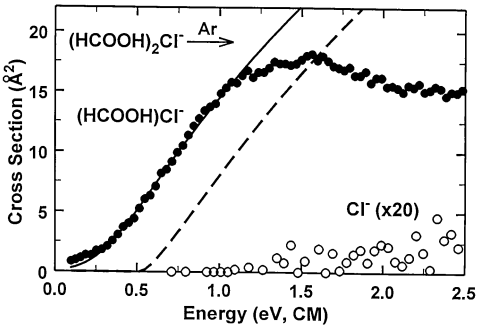

Fig. 4. Cross section for collision-induced dissociation of $(HCOOH)_2Cl^-$ as a function of energy in the center-of-mass frame. The solid line is the optimized fit to the data, and the dashed line is the fit without internal energy effects or translational energy broadening. See text for discussion of fitting procedures.

$$(HCOOH)_2X^- \rightarrow 2\,HCOOH + X^- \quad (6)$$

The Eq. (2) fitting parameters for fits to the data are given in Table 1, and the fits are shown in Figs. 1–6 as well. The dissociation thresholds correspond to the bond energies at 0 K, since the effects of reactant and product internal energy are included in the fitting procedure. The reported uncertainties in the reaction thresholds are derived from the standard deviation of fits to individual data sets, the uncertainty in the reactant internal energy, and the uncertainty in the energy scale ($\pm$0.15 eV lab).

The 0 K bond energies can be converted into 298 K bond enthalpies using the heat capacities of the reactants and products. The heat capacities calculated using the AM1 frequencies give 298 K bond enthalpies that are 2 kJ mol^{-1} higher for the $(HCOOH)X^-$ systems and 3 kJ mol^{-1} lower for the $(HCOOH)_2X^-$ systems. The sensitivity of these correction factors to the calculated vibrational frequencies is estimated to be 1 kJ mol^{-1} by assuming a consistent 10% error in all the frequencies in a molecule. The resulting thermochemistry is listed in Table 2.

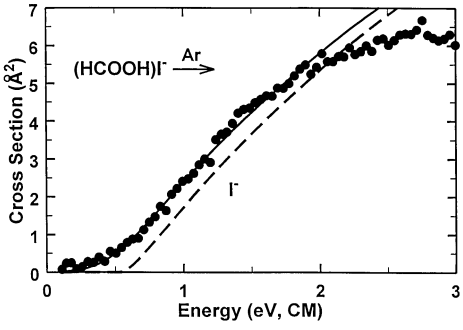

Fig. 3. Cross section for collision-induced dissociation of $(HCOOH)I^-$ as a function of energy in the center-of-mass frame. The solid line is the optimized fit to the data, and the dashed line is the fit without internal energy effects or translational energy broadening. See text for discussion of fitting procedures.

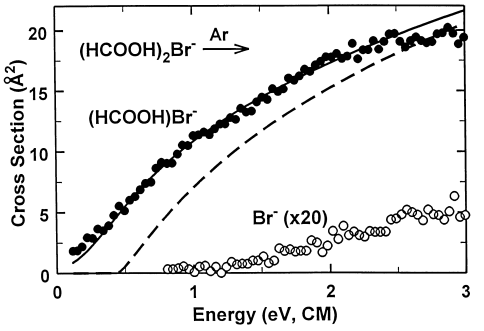

Fig. 5. Cross section for collision-induced dissociation of $(HCOOH)_2Br^-$ as a function of energy in the center-of-mass frame. The solid line is the optimized fit to the data, and the dashed line is the fit without internal energy effects or translational energy broadening. See text for discussion of fitting procedures.

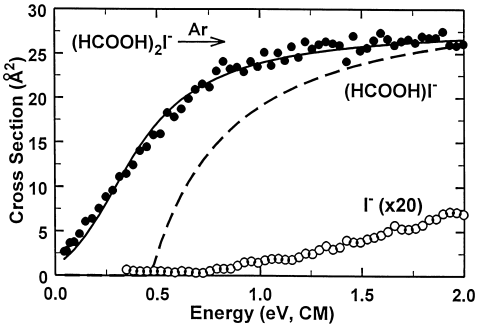

Fig. 6. Cross section for collision-induced dissociation of $(HCOOH)_2I^-$ as a function of energy in the center-of-mass frame. The solid line is the optimized fit to the data, and the dashed line is the fit without internal energy effects or translational energy broadening. See text for discussion of fitting procedures.

4. Discussion

4.1. Comparison to previous work

The results from three previous studies of $(HCOOH)_yX^-$ systems are also given in Table 2. The three values for D(HCOOH–Cl^-) are in good agreement. In contrast, the present value for D(HCOOH–I^-) is significantly lower than the previously reported value. This issue is discussed further below.

The $(HCOOH)_2Cl^-$ bond strength has the largest disparity. The previously reported bond strength is even stronger than D(HCOOH–Cl^-). The large cross section and very low apparent threshold in the present results are not consistent with this value. The higher bond strength is also inconsistent with the corresponding values for $(HCOOH)_2Br^-$ and $(HCOOH)_2I^-$. Łuczynski et al. also measured D[$(HCOOH)_2Cl^-$–HCOOH] = 93 ± 11 kJ mol^{-1}. A small amount of $(HCOOH)_3Cl^-$ is observed in the present experiments. This suggests that the binding energy is around 40 kJ mol^{-1}, the binding energy of the weakest clusters typically observed in room-temperature flowing afterglow instruments. The cause of the discrepancy between the two sets of $(HCOOH)_yCl^-$ thermochemistry is not known.

Table 1.
Fitting parameters for CID of $(HCOOH)_yX^-$ [a]

X	y	E_T(eV)	n
Cl	1	1.18 ± 0.10	1.3 ± 0.2
Cl	2	0.52 ± 0.09	1.5 ± 0.3
Br	1	0.72 ± 0.07	1.7 ± 0.3
Br	2	0.44 ± 0.07	1.4 ± 0.3
I	1	0.54 ± 0.09	1.6 ± 0.2
I	2	0.47 ± 0.10	1.2 ± 0.2

[a]See text for discussion of fitting parameters.

Table 2.
Bond dissociation energies for $(HCOOH)_yX^-$ complexes[a]

X	y	This work (0 K)	This work (298 K)	Literature values	AM1 calcs[f]
Cl	1	114 ± 9	116 ± 9	115 ± 8[b] 107[c]	92
Cl	2	50 ± 9	47 ± 9	143 ± 13[d]	59
Br	1	70 ± 7	72 ± 7		83
Br	2	43 ± 7	40 ± 7		51
I	1	52 ± 9	54 ± 9	79 ± 4[e]	72
I	2	45 ± 9	42 ± 9		42

[a]Values in kJ mol^{-1}.
[b][21].
[c][23].
[d][25].
[e][22].
[f]See text.

4.2. Correlation with acidity

A correlation between anion–neutral hydrogen bond strength and the gas-phase acidity of the neutral has been previously noted [20,21,23,26]. This correlation is better within groups of similar molecules, and the previous work indicates that oxyacids including water, alcohols, and carboxylic acids can be considered together [21,23,33]. The new data are consistent with the results expected from the correlation. A linear regression fit to the iodine data suggests that the correct value for D(HCOOH–I^-) is between the two experimental results.

4.3. Correlation with acidity and electronegativity

Larson and McMahon [34] extended the above work by deriving an empirical relationship correlating hydrogen bond strengths in YH–X^- systems to both the acidities of the species involved, D(X^-–H^+) and

$D(Y^-–H^+)$, and the electronegativities of the hydrogen bonding atoms, $\chi(X)$ and $\chi(Y)$. This empirical relationship was given as Eq. (7), where the units for bond energies are kcal mol^{-1}.

$$D(YH–X^-) = (443 - D(Y^-–H^+))[(\chi(X) + \chi(Y))/12 + D(X^-–H^+)/300 - 1.4] \quad (7)$$

The average difference between experimental halide affinities [17,35] for oxyacids and affinities predicted using this method is 7.7 kJ mol^{-1}, indicating that Eq. (7) should be appropriate for the present data. The correlation predicts bond strengths of 104, 83, and 60 kJ mol^{-1} for $(HCOOH)X^-$, with X = Cl, Br, and I. These predictions and the experimental results agree within the expected uncertainties. Again, the predicted value for $D(HCOOH–I^-)$ lies between the two experimental results.

4.4. AM1 calculations

AM1 semiempirical calculations are moderately successful at reproducing hydrogen bond strengths [36–38]. AM1 bond strengths are given in Table 2. The calculated $HCOOH–Cl^-$ bond strength is lower than the experimental values by 15–24 kJ mol^{-1}. The other results are in better agreement, with the calculated values typically higher than experiment. The calculated value for $(HCOOH)I^-$ lies between the two experimental values. A comparison of AM1 and experimental bond strengths for other oxyacids indicates that AM1 calculated bond strengths are low by an average of 11%.

While the $(HCOOH)X^-$ bond strengths decline from X = Cl to I, the three measured bond strengths in $(HCOOH)_2X^-$ are nearly equal. Although the effect of varying X should decline with increasing cluster size, the near lack of a trend is somewhat surprising. The fitting parameter *n*, which is related to the efficiency of energy deposition upon collisional activation, is expected to be nearly independent of X. In the present data, the best fits for reaction (5) give average *n* values of 1.5 ± 0.3, 1.4 ± 0.3, and 1.2 ± 0.2. Fitting data for all three $(HCOOH)_2X^-$ molecules with *n* fixed at 1.4 gives bond energies of 50, 40, and 36 kJ mol^{-1} for X = Cl, Br, and I, respectively. Thus, a declining trend in the bond strengths may be hidden within the error limits of the individual measurements.

4.5. $HCOOH–I^-$

The two measurements for $D(HCOOH–I^-)$ differ by 25 ± 10 kJ mol^{-1}. The values for this bond strength predicted by the two correlations and the semiempirical calculations all come out between the two experimental values. Thus, the actual value is plausibly near 70 kJ mol^{-1}, approximately two standard deviations from both of the measurements.

The *cis* isomer of formic acid is higher in energy than the *trans* isomer by 16 kJ mol^{-1} [39]. Based on electrostatic calculations, Caldwell and Kebarle predicted that the formic acid–halide clusters have a *cis* geometry, which would enable the C–H and C═O dipoles to align favorably with the negatively charged halide [22]. This prediction is borne out in the AM1 calculations, where the *cis* isomers of $(HCOOH)X^-$ are lower in energy by 13, 9, and 7 kJ mol^{-1} for X = Cl, Br, and I. It is possible that these additional interactions could make the formic acid–anion bonds stronger than predicted by the empirical correlations. However, the calculated Mulliken and electrostatic charges on the atoms in these clusters indicate that the C–H dipole is negligible, suggesting that the *cis* geometry is dictated more by avoiding a repulsive interaction with the C═O dipole.

Acknowledgements

The authors thank Professor Peter Armentrout and co-workers for use of the CRUNCH data analysis program.

References

[1] Y. Marcus, Ion Properties, Marcel Dekker: New York, 1997.
[2] A.W. Castlemen Jr., K.H. Bowen Jr., J. Phys. Chem. 100 (1996) 12911.

[3] M. Meot-ner (Mautner), S. Scheiner, W.O. Yu, J. Am. Chem. Soc. 120 (1998) 6980, and refs. therein.
[4] J.V. Coe, J. Phys. Chem. 101 (1997) 2055.
[5] G.A. Jeffrey, An Introduction to Hydrogen Bonding, Oxford University Press, Oxford, 1997.
[6] S. Scheiner, Hydrogen Bonding: A Theoretical Perspective, Oxford University Press, Oxford, 1997.
[7] R.G. Keesee, A.W. Castleman Jr., J. Phys. Chem. Ref. Data 15 (1986) 1011.
[8] P. Kebarle, Annu. Rev. Phys. Chem. 28 (1977) 445.
[9] M. Arshadi, R. Yamdagni, P. Kebarle, J. Phys. Chem. 74 (1970) 1475.
[10] I. Džidić, P. Kebarle, J. Phys. Chem. 74 (1970) 1466.
[11] M. Born, Z. Phys. 1 (1920) 15.
[12] W.M. Latimer, K.S. Pitzer, C.M. Slansky, J. Chem. Phys. 7 (1939) 108.
[13] G.W. Caldwell, J.A. Masucci, M.G. Ikonomou, Org. Mass Spectrom. 24 (1989) 8.
[14] G. Markovich, S. Pollack, R. Ginger, O. Cheshnovsky, J. Chem. Phys. 101 (1994) 9344.
[15] R. Yamdagni, J.D. Payzant, P. Kebarle, Can. J. Chem. 51 (1973) 2507.
[16] F.E. Wilkinson, M. Peschke, J. Szulejko, T.B. McMahon, Int. J. Mass Spectrom. 175 (1998) 225.
[17] B. Bogdanov, M. Peschke, D.S. Tonner, J.E. Szulejko, T.B. McMahon, Int. J. Mass Spectrom., submitted.
[18] R.G. Keesee, A.W. Castelman Jr., Chem. Phys. Lett. 73 (1980) 2195.
[19] P.G. Wenthold, R.R. Squires, J. Phys. Chem. 99 (1995) 2002.
[20] R. Yamdagni, P. Kebarle, J. Am. Chem. Soc. 93 (1971) 7139.
[21] M.A. French, S. Ikuta, P. Kebarle, Can. J. Chem. 60 (1982) 1907.
[22] G. Caldwell, P. Kebarle, J. Am. Chem. Soc. 106 (1984) 967.
[23] J.W. Larson, T.B. McMahon, J. Am. Chem. Soc. 106 (1984) 517.
[24] M. Meot-ner (Mautner), L.W. Sieck, J. Am. Chem. Soc. 108 (1986) 7525.
[25] Z. Łuczynski, S. Włodek, H. Wincel, Int. J. Mass. Spectrom. Ion Phys. 26 (1978) 103.
[26] J.W. Larson, T.B. McMahon, J. Am. Chem. Soc. 105 (1983) 2944.
[27] K. Do, T.P. Klein, C.A. Pommerening, L.S. Sunderlin, J. Am. Soc. Mass Spectrom. 8 (1997) 688.
[28] (a) K.M. Ervin, P.B. Armentrout, J. Chem. Phys. 83 (1985) 166; (b) M.T. Rodgers, K.M. Ervin, P.B. Armentrout, ibid. 106 (1997) 4499.
[29] A.T. Pudzianowski, J. Phys. Chem. 100 (1996) 4781.
[30] PC SPARTAN, Wavefunction Inc., Irvine, CA, 1996.
[31] R.L. Redington, J. Mol. Spectrosc. 65 (1977) 171.
[32] (a) S.K. Loh, D.A. Hales, L. Lian, P.B. Armentrout, J. Chem. Phys. 90 (1989) 5466; (b) R.H. Schultz, K.C. Crellin, P.B. Armentrout, J. Am. Chem. Soc. 113 (1991) 8590.
[33] G.J.C. Paul, P. Kebarle, Can. J. Chem. 68 (1990) 2070.
[34] J.W. Larson, T.B. McMahon, J. Am. Chem. Soc. 109 (1987) 6230.
[35] NIST Standard Reference Database #69, November 1998 release, W.G. Mallard, P.J. Linstrom (Eds.) (http://webbook.nist.gov).
[36] M.J.S. Dewar, E.G. Zoebisch, E.F. Healy, J.J.P. Stewart, J. Am. Chem. Soc. 107 (1985) 3902.
[37] D. Banerjee, A.K. Chandra, M. Banerjee, S. Bagchi, J. Mol. Struct. 343 (1995) 167.
[38] W.D. Chandler, K.E. Johnson, J.L.E. Campbell, Inorg. Chem. 34 (1995) 4943.
[39] W.H. Hocking, Z. Naturforsch. 31A (1976) 1113.